

A TENTATIVE DETECTION OF THE COSMIC INFRARED BACKGROUND AT 3.5 μm FROM *COBE*/DIRBE OBSERVATIONS

E. Dwek¹, R. G. Arendt²

ABSTRACT

Foreground emission and scattered light from interplanetary dust (IPD) particles and emission from Galactic stellar sources are the greatest obstacles for determining the cosmic infrared background (CIB) from diffuse sky measurements in the ~ 1 to $5 \mu\text{m}$ range. We use ground-based observational limits on the K-band intensity of the CIB in conjunction with skymaps obtained by the Diffuse Infrared Background Experiment (DIRBE) on the *Cosmic Background Explorer* (*COBE*) satellite to reexamine the limits on the CIB at 1.25, 3.5, and $4.9 \mu\text{m}$. Adopting a CIB intensity of $7.4 \text{ nW m}^{-2} \text{ sr}^{-1}$ at $2.2 \mu\text{m}$, and using the $2.2 \mu\text{m}$ DIRBE skymap from which the emission from IPD cloud has been subtracted, we create a spatial template of the Galactic stellar contribution to the diffuse infrared sky. This template is then used to subtract the contribution of the diffuse Galactic stellar emission from the IPD-emission-subtracted DIRBE skymaps at 1.25, 3.5, and $4.9 \mu\text{m}$. The DIRBE $100 \mu\text{m}$ data are used to estimate the small contribution of emission from interstellar dust at 3.5 and $4.9 \mu\text{m}$. Our method significantly reduces the errors associated with the subtraction of Galactic starlight, leaving only the IPD emission component as the primary obstacle for the detection of the CIB at these wavelengths. The analysis leads to a tentative detection of the CIB at $3.5 \mu\text{m}$ with an intensity of $\nu I_\nu = \{9.9 + 0.312[\nu_0 I_{CIB}(\nu_0) - 7.4]\} \pm 2.9 \text{ nW m}^{-2} \text{ sr}^{-1}$, where $\nu_0 I_{CIB}(\nu_0)$ is the CIB intensity at $2.2 \mu\text{m}$ in units of $\text{nW m}^{-2} \text{ sr}^{-1}$. The analysis also yields new upper limits (95% CL) on the CIB at 1.25 and $4.9 \mu\text{m}$ of 68 and $36 \text{ nW m}^{-2} \text{ sr}^{-1}$, respectively. The cosmological implications of these results are discussed in the paper.

Subject headings: cosmology:observations - diffuse radiation - infrared: general

1. INTRODUCTION

Determination of the cosmic infrared background (CIB) from diffuse sky measurements is greatly hampered by the presence of foreground emission and scattered light from the interplanetary dust (IPD) cloud, and emission from discrete and unresolved stellar components in our Galaxy, and from dust in the interstellar medium (ISM). In a recent publication, Hauser et al. (1998) presented the results of the search for the (CIB) in the 1.25 to $240 \mu\text{m}$ wavelength region that was conducted with the Diffuse Infrared Background Experiment (DIRBE) on the *Cosmic Background Explorer* (*COBE*) satellite. Careful subtraction of foreground emission from the IPD cloud (Kelsall et al. 1998) and from stellar and interstellar

¹Laboratory for Astronomy and Solar Physics, Code 685, NASA/Goddard Space Flight Center, Greenbelt, MD 20771. e-mail address: eli.dwek@gssc.nasa.gov

²Raytheon STX, Code 685, NASA/Goddard Space Flight Center, Greenbelt, MD 20771

Galactic emission components (Arendt et al. 1998) revealed a residual emission component in the DIRBE skymaps that, after detailed analysis of the random and systematic uncertainties, was consistent with a positive signal at 100, 140, and 240 μm . Subsequent rigorous tests showed that only the 140 and 240 μm signals were isotropic, a strict requirement for their extragalactic origin. Only upper limits for the CIB intensity were given for $\lambda = 1.25 - 60 \mu\text{m}$, where the CIB detection was hindered by residual emission from the IPD cloud. In the 1.25 to 4.9 μm wavelength region, uncertainties in the subtraction of the Galactic stellar component contributed to the uncertainties as well. The upper limits on the CIB determined by Hauser et al. (1998) can be found in Table 2.

In this paper we use a new empirical model for the Galactic stellar emission in order to reduce the uncertainties attributed by the DIRBE team to the removal of this component. Our analysis relies on the modeling and error analysis of the IPD and the ISM contributions to the diffuse emission presented by Kelsall et al. (1998) and Arendt et al. (1998). We use the DIRBE 1.25, 2.2, 3.5, and 4.9 μm all sky maps from which the emission from interplanetary (zodiacal) dust has been subtracted (Kelsall et al. 1998) as a starting point in our analysis. The intensity, $I_G(\lambda_j)$, of these maps should, in principle, contain only the Galactic emission (starlight and ISM emission) and the CIB. Assuming that the CIB is somehow determined from other independent observations at wavelength λ_0 , then subtraction of this background, $I_{CIB}(\lambda_0)$, from the corresponding DIRBE skymap will create a spatial template of the Galactic emission at this wavelength. At $\lambda_0 = 2.2 \mu\text{m}$, emission from the ISM is negligible, and this template corresponds to the Galactic starlight. Correlation of this stellar template map, $S_\nu(\lambda_0)$, with the zodi-subtracted skymaps should yield a straight line with a slope of $S_\nu(\lambda_j)/S_\nu(\lambda_0)$ corresponding to the average Galactic stellar flux ratio, and a non-zero intercept at zero $S_\nu(\lambda_0)$ intensity, which one can identify as the CIB contribution to $I_G(\lambda_j)$ after a small correction for the ISM emission is subtracted at 3.5 and 4.9 μm .

The method is based on the assumption that the difference map $I_G(\lambda_0) - I_{CIB}(\lambda_0)$ is a good representation of $S_\nu(\lambda_0)$, the intensity map of the Galactic stellar contribution at λ_0 . Correlation of $S_\nu(\lambda_0)$ with maps at other wavelengths will allow the identification and removal of the stellar emission at those wavelengths. For $I_{CIB}(\lambda_0)$ we use the recently determined ground-based K-band ($\lambda = 2.2 \mu\text{m}$) galaxy counts, which give a strict lower limit of $7.4 \text{ nW m}^{-2} \text{ sr}^{-1}$ to the CIB intensity at that wavelength (e.g. Gardner 1996). Plots of the K-band contribution to the CIB versus the magnitude (e.g. Pozzetti et al. 1998) show a decrease in the intensity at faint magnitudes, suggesting that the contribution of faint galaxies to the integrated light is small. We therefore adopt the above intensity as the nominal value for the CIB at 2.2 μm , and explicitly state the dependence of our results on this value.

We apply the method to regions in the DIRBE skymaps that were identified in the DIRBE analysis as high quality (HQ) regions where errors in subtractions of the foreground emission are expected to be small (Hauser et al. 1998; see also §2.1 below). The results show an extremely good correlation between $S_\nu(2.2 \mu\text{m})$ and $S_\nu(\lambda_j)$ ($\lambda_j = 1.25, 3.5, \text{ and } 4.9 \mu\text{m}$), characterized by a narrow dispersion and a positive intercept. Concentrating on HQB, the high quality region emphasized in the analysis by the DIRBE team, we identify the uncertainties in the method as the difference between the intercept in HQBN and HQBS, the northern and southern sections of HQB. These uncertainties are small compared with those associated with the subtraction of the Faint Source Model (FSM) which the DIRBE team had used to characterize the contribution of unresolved Galactic stellar sources (Arendt et al. 1998). At 1.25 and 4.9 μm , uncertainties in the residuals are about equally divided between the systematic errors in the subtraction of the zodiacal light and the subtraction of the FSM contributions to the emission. So a priori we do not expect our method to result in a significant reduction in the uncertainties in the CIB determination at these wavelengths. However, at 3.5 μm , uncertainties in the Hauser et al. (1998) results are dominated by systematic errors

in the FSM, which are significantly larger than the errors in the proposed method. With this reduction of uncertainties, our analysis yields a positive detection of the CIB at $3.5 \mu\text{m}$. The values derived for the CIB in different regions of the sky falls within the uncertainties, providing a simple test for their isotropic character.

2. ANALYSIS

2.1. An Empirical Model of Galactic Starlight

As described in the Introduction, we adopt a value of $\nu I_{CIB}(2.2 \mu\text{m}) = 7.4 \text{ nW m}^{-2} \text{ sr}^{-1}$ for the CIB intensity in the K–band, and create a difference map $S_\nu(2.2 \mu\text{m}) \equiv I_G(2.2 \mu\text{m}) - I_{CIB}(2.2 \mu\text{m})$, which we identify as the spatial template of the Galactic stellar contribution to the diffuse IR sky. We chose for our analysis high quality (HQ) regions of the sky, identified as such for their location at high Galactic latitudes (b) and ecliptic latitudes (β), in which the contributions from the Galactic and zodiacal emission components are relatively small compared to other regions of the sky. HQA is a region encompassing 8780 deg^2 of the sky at $|b| > 30^\circ, |\beta| > 25^\circ$, including sections in both the northern and southern hemispheres. The HQB region is a smaller area of 854 deg^2 contained within HQA at $|b| > 60^\circ, |\beta| > 45^\circ$. Both HQ regions exclude several locations where the ISM intensity is strong, $I_{ISM} > 0.2 \text{ MJy/sr}$.

Figure 1 shows the correlation of $\nu I_G(\lambda_j)$ versus $\nu S_\nu(2.2 \mu\text{m})$ within HQB for $\lambda_j = 1.25, 3.5, \text{ and } 4.9 \mu\text{m}$. A linear least–squares fit was performed to derive the intercepts and slopes of these correlations in addition to the correlation coefficients. Results of these fits for the HQA and HQB regions and their north and south subregions (e.g. HQAN, HQAS) are presented in Table 1. The slopes of the correlations in Figure 1 and Table 1 represent the colors of stellar emission. Most of this emission is unresolved (the brightest resolved sources lie outside the ranges displayed in Figure 1 and were excluded from the fit), but the colors are still a very good match to those of M and K giants as shown in Figure 2 of Arendt et al. (1994). The intercepts of the correlations, $I_{int}(\lambda_j)$, give the remaining intensity of any emission unassociated with Galactic starlight. At 3.5 and $4.9 \mu\text{m}$ this includes emission from the ISM. Following Arendt et al. (1998), we estimate and remove the mean level of this ISM emission by scaling the average intensity of the $100 \mu\text{m}$ ISM emission seen by DIRBE in these regions by factors of 0.00183 and 0.00292 at 3.5 and $4.9 \mu\text{m}$ respectively. The resulting contribution of the ISM to the emission in each band is also listed in Table 1.

2.2. Uncertainties

Three sources of errors contribute to the uncertainties in the derived intensity of the CIB. The first consists of the uncertainties in the residuals of the zodiacal emission, σ_Z , contained in the DIRBE skymaps $I_G(\lambda_j)$, ($\lambda_j = 1.25, 3.5, \text{ and } 4.9 \mu\text{m}$), as well as the $S_\nu(2.2 \mu\text{m})$ difference map. The second uncertainty is that associated with the subtraction of the emission from the ISM. The third results from the uncertainty in the value of the intercept, denoted hereafter as σ_{int} . The total uncertainty in the residual emission is given by:

$$\begin{aligned} \sigma_{res}(\lambda_j) &= [\sigma_Z^2(\lambda_j) + \sigma_{ISM}^2(\lambda_j) + [S_\nu(\lambda_j)/S_\nu(2.2 \mu\text{m})\sigma_Z(2.2 \mu\text{m})]^2 + \sigma_{int}^2(\lambda_j)]^{1/2} \\ &\equiv [\sigma_Z^2(\lambda_j) + \sigma_{ISM}^2(\lambda_j) + \sigma_{star}^2(\lambda_j)]^{1/2} \end{aligned} \quad (1)$$

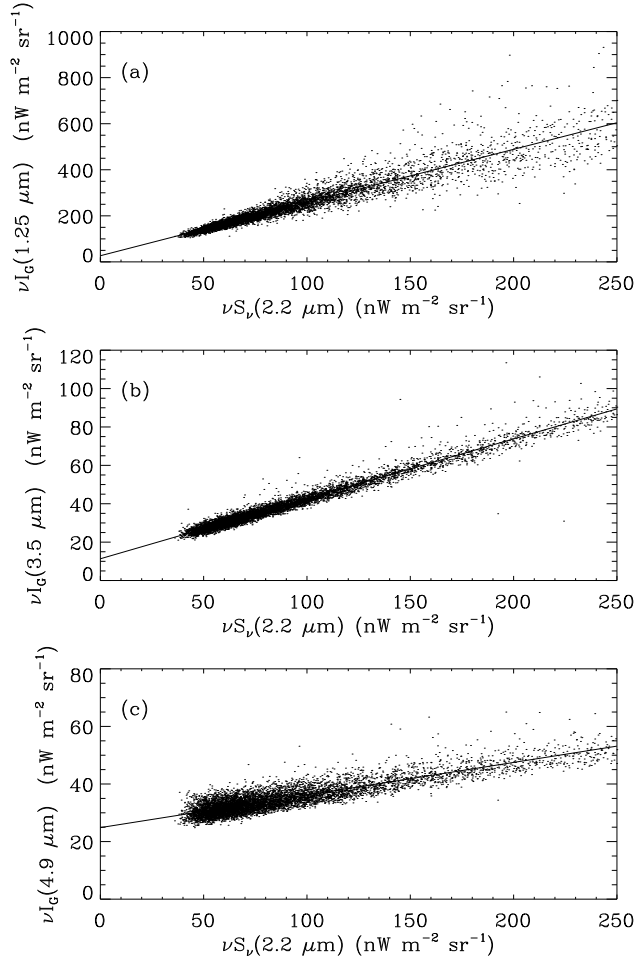


Fig. 1.— Correlation plots of $\nu S_\nu(2.2 \mu\text{m})$ vs. (a) $\nu I_G(1.25 \mu\text{m})$, (b) $\nu I_G(3.5 \mu\text{m})$, and (c) $\nu I_G(4.9 \mu\text{m})$ for the HQB region. The straight lines are linear least-squares fits to the data with parameters as indicated in Table 1.

where $\sigma_{star}(\lambda_j) \equiv [S_\nu(\lambda_j)/S_\nu(2.2 \mu\text{m})\sigma_Z(2.2 \mu\text{m})]^2 + \sigma_{int}^2(\lambda_j)$, is the total uncertainty associated with our empirical stellar model. Table 2 lists the total uncertainty, $\sigma_{res}(\lambda_j)$, and the various contributions to the uncertainty in the value of $I_{res}(\lambda_j)$. The values of $\sigma_Z(\lambda_j)$ and $\sigma_{ISM}(\lambda_j)$ were taken from Arendt et al. (1998; Table 6), and the value of $\sigma_{int}(\lambda_j)$ was taken to be equal to the absolute value of the difference in the value of $I_{int}(\lambda_j)$ between in HQBN and HQBS. Also listed in the table are the systematic errors, $\sigma_{FSM}(\lambda_j)$, derived by Arendt et al. (1998; Table 6) due to uncertainties in the subtraction of the FSM. Comparison of $\sigma_{star}(\lambda_j)$ to the error associated with the FSM illustrates the effectiveness of our method in reducing the uncertainties in removing the Galactic stellar emission component.

2.3. Residual Intensities

The residual intensity after subtraction of the IPD, stellar, and ISM foregrounds, is given by: $I_{res} = I_{int} - I_{ISM}$. Following Hauser et al. (1998) we derive our results from the analysis of the HQB region, which can be summarized as:

$$\begin{aligned} \nu I_{res}(\text{nW m}^{-2} \text{sr}^{-1}) &= 26.9 + 2.31 \Delta_{CIB}(2.2 \mu\text{m}) \pm 20.6 \quad \text{for } \lambda = 1.25 \mu\text{m} \\ &= 9.9 + 0.312 \Delta_{CIB}(2.2 \mu\text{m}) \pm 2.9 \quad \text{for } \lambda = 3.5 \mu\text{m} \\ &= 23.3 + 0.113 \Delta_{CIB}(2.2 \mu\text{m}) \pm 6.4 \quad \text{for } \lambda = 4.9 \mu\text{m} \end{aligned} \quad (2)$$

where the quoted errors represent 1σ uncertainties, and $\Delta_{CIB}(2.2 \mu\text{m}) \equiv [I_{CIB}(2.2 \mu\text{m}) - 7.4]$ represents the difference in the actual value of the CIB at $2.2 \mu\text{m}$ (in $\text{nW m}^{-2} \text{sr}^{-1}$) and the nominal value adopted in our model. Values of $\nu I_{res}(\nu)$ for $\Delta_{CIB}(2.2 \mu\text{m}) = 0$ are listed in Table 2. Only the 3.5 and 4.9 μm residuals are positive ($> 3\sigma$) and therefore potential detections of the CIB.

2.4. Isotropy Tests

We tested the residual intensities in the 3.5 and 4.9 μm bands for isotropy, an expected property of the CIB. Table 1 shows that the residual 3.5 μm emission is isotropic, as evident from the agreement between the mean intensities in the various HQ regions. However, a more detailed analysis shows the presence of a low-level large scale gradient. This gradient is caused by residual emission from IPD particles. This gradient would have been undetected in the analysis of Hauser et al. (1998) using the FSM to subtract the Galactic stellar emission. The reduction in this gradient from the level found by Hauser et al. (1998) to its present level is the result of our more accurate subtraction of the stellar emission component. Without the existence of this weak gradient, the residual would classify as a definite detection of the CIB. Instead, we conservatively regard this result as a tentative detection of the CIB at 3.5 μm .

The same gradient seen in the 3.5 μm image is significantly stronger in the 4.9 μm residual map, and is responsible for the larger dispersion in the mean intensities in the various HQ regions. We therefore consider the 4.9 μm result as only an upper limit.

3. DISCUSSION

Figure 2 shows the current limits on and tentative detection of the extragalactic background light (EBL) in the 0.1 to 10 μm wavelength region. The filled squares represent the detections at 0.36, 0.45, 0.67, and 0.81 μm from background fluctuations analysis of the Hubble Deep Field (Pozzetti et al. 1998). The total EBL intensity in the 0.36 to 3.5 μm wavelength region is $16 \text{ nW m}^{-2} \text{sr}^{-1}$, about equal to the total integrated CIB intensity in the 140 to 1000 μm region (Hauser et al. 1998; Fixsen et al. 1998; Dwek et al. 1998).

Figure 2 compares several model predictions to the observational constraints. The solid line represents the model of Franceschini et al. (1997), and the dashed line represents that calculated by Malkan & Stecker (1998). Both models are consistent with the tentative 3.5 μm detection. However, they are incomplete with regard to their EBL prediction at shorter wavelengths. The dotted line represents two models calculated by Dwek et al. (1998) in which the UV and optically determined cosmic star formation rate presented

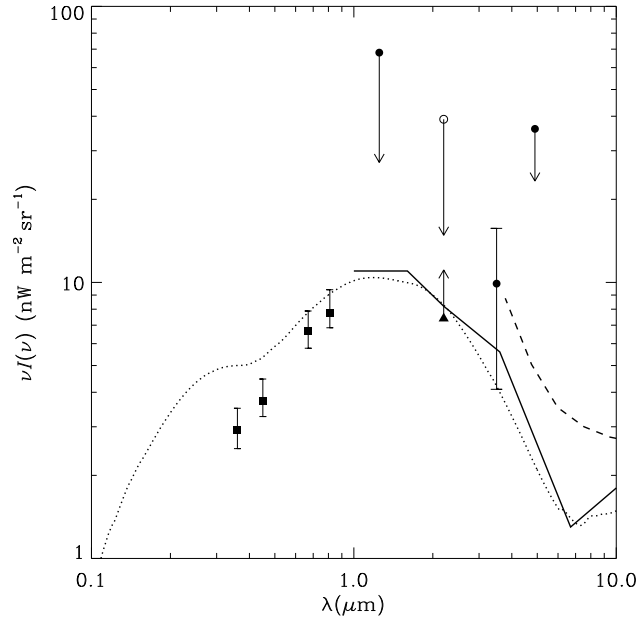


Fig. 2.— UV determination of the EBL and our *COBE*/DIRBE limits and tentative $3.5 \mu\text{m}$ detection (solid circles) are compared to select model predictions: Franceschini et al. (1997; solid line), Malkan & Stecker (1998; dashed line). The dotted line represents model *ED* from Dwek et al. (1998) scaled up by a factor of 1.2. The solid squares represent HDF detections by Pozzetti et al. (1998), the solid triangle represents the $2.2 \mu\text{m}$ lower limit from galaxy counts (Gardner 1996), and the open circle is the DIRBE upper limit at $2.2 \mu\text{m}$ (Hauser et al. 1998).

by Madau et al. (1998) was augmented by hidden starbursts at either $z \approx 1.5$ (model *ED*) or by hidden starbursts at high redshifts (model *RR*). The models give similar results in the 0.1 to $10 \mu\text{m}$ wavelength regions, and were scaled up by a factor of 1.2 in order to provide a better fit to the tentative $3.5 \mu\text{m}$ detection. The models produce however an excess flux at 0.36 and $0.45 \mu\text{m}$ requiring some modifications in the model assumptions.

Most models to date have concentrated on predicting the EBL at mid- and far-IR wavelengths, and appear to be incomplete in the UV and near-IR regions of the spectrum. Our tentative detection of the CIB at $3.5 \mu\text{m}$ adds an important new constraint on CIB models in this wavelength region.

We acknowledge helpful conversations with Jonathan Gardner and Harvey Moseley, and thank Janet Weiland, Tom Kelsall, and Dave Leisawitz for their useful comments on the manuscript. This research was supported by the NASA Astrophysical Theory Program NRA97-12-OSS-098.

REFERENCES

- Aaronson, M. 1978, *ApJ*, 221, L108
 Arendt, R. G. et al. 1994, *ApJ*, 425, L85

- Arendt, R. G. et al. 1998, ApJ, in press (astro-ph/9805323)
- Dwek, E. et al. 1998, ApJ, in press (astro-ph/9806129)
- Fixsen, D. J., Dwek, E., Mather, J. C., Bennett, C. L., & Shafer, R. A. 1998, ApJ, in press (astro-ph/9803021)
- Franceschini, A. et al. 1997, in *The Far InfraRed and Submillimetre Universe*, ed. A. Wilson (Noordwijk: ESA Publication Division), 159
- Gardner, J. P. 1996, in *Unveiling the Cosmic Infrared Background*, ed. E. Dwek (New York: AIP Press), p. 127
- Hauser, M. G. et al. 1998, ApJ, in press (astro-ph/9806167)
- Kelsall, T. J., et al. 1998, ApJ, in press (astro-ph/9806250)
- Madau, P., Pozzetti, L., & Dickinson, M. 1998, ApJ, 498, 106
- Malkan, M. A., & Stecker, F. W. 1998, ApJ, 496, 13
- Pozzetti, L., Madau, P., Ferguson, H. C., Zamorani, G., & Bruzual, G. A. 1998, MNRAS, in press (astro-ph/9803144)

Table 1. Results of Correlations Identifying Emission Components

Region	Wavelength (μm)	Number of pixels	Correlation Coefficient	Slope = $\frac{\nu S_\nu(\lambda_j)}{\nu S_\nu(2.2 \mu\text{m})}$	Intercept = $\nu I_{int}(\lambda_j)$ ($\text{nW m}^{-2} \text{sr}^{-1}$)	$\nu I_{ISM}(\lambda_j)$ ($\text{nW m}^{-2} \text{sr}^{-1}$)
HQB	1.25	7460	0.95	2.310 ± 0.009	26.9 ± 0.8	...
HQBN	1.25	3643	0.95	2.315 ± 0.012	28.0 ± 1.1	...
HQBS	1.25	3817	0.95	2.311 ± 0.013	25.3 ± 1.3	...
HQA	1.25	73917	0.96	2.288 ± 0.002	30.4 ± 0.3	...
HQAN	1.25	37353	0.96	2.302 ± 0.003	30.7 ± 0.4	...
HQAS	1.25	36564	0.96	2.280 ± 0.004	29.6 ± 0.4	...
HQB	3.5	7461	0.98	0.3123 ± 0.0007	11.34 ± 0.07	1.4
HQBN	3.5	3643	0.98	0.3112 ± 0.0010	10.93 ± 0.09	1.2
HQBS	3.5	3818	0.98	0.3111 ± 0.0009	11.93 ± 0.09	1.5
HQA	3.5	73905	0.98	0.3141 ± 0.0002	11.95 ± 0.03	2.2
HQAN	3.5	37349	0.98	0.3125 ± 0.0003	11.69 ± 0.04	2.1
HQAS	3.5	36556	0.98	0.3142 ± 0.0003	12.36 ± 0.04	2.3
HQB	4.9	7461	0.88	0.1133 ± 0.0007	24.85 ± 0.07	1.6
HQBN	4.9	3643	0.91	0.1116 ± 0.0008	23.89 ± 0.08	1.4
HQBS	4.9	3818	0.88	0.1101 ± 0.0010	26.19 ± 0.10	1.7
HQA	4.9	73901	0.66	0.0987 ± 0.0004	28.31 ± 0.05	2.5
HQAN	4.9	37348	0.72	0.1015 ± 0.0005	26.96 ± 0.06	2.4
HQAS	4.9	36553	0.61	0.0922 ± 0.0006	30.10 ± 0.07	2.6

Table 2. Residual Emission and Uncertainties^a

$\lambda(\mu\text{m})$	1.25	2.2	3.5	4.9
σ_Z	15.	6.	2.	6.
σ_{ISM}	0.4	0.6
σ_{int}	2.7	...	0.70	2.0
σ_{res}	20.6	...	2.86	6.39
σ_{star}	14.1	...	2.0	2.1
σ_{FSM}	15.	10.	6.	5.
$\nu I_{res}(HQB)$	26.6 ± 20.6	...	9.9 ± 2.9	23.3 ± 6.4
Isotropy	no	assumed	weak	no
νI_{CIB}^b	< 68	7.4 (assumed)	9.9 ± 2.9	< 36

^aAll values are given in units of $\text{nW m}^{-2} \text{sr}^{-1}$.

^bFor comparison, νI_{CIB} intensities from Hauser et al. (1998) are: < 75 , < 39 (14.9 ± 12), < 23 (11.4 ± 6), and $< 44 \text{ nW m}^{-2} \text{sr}^{-1}$ at 1.25, 2.2, 3.5, and 4.9 μm , respectively.